ELSEVIER

Mechanisms of Development 69 (1997) 169–181

Identification of the vertebrate Iroquois homeobox gene family with overlapping expression during early development of the nervous system

Antje Bosse[a,*], Armin Zülch[a], May-Britt Becker[a], Miguel Torres[b], José Luis Gómez-Skarmeta[c,d], Juan Modolell[d], Peter Gruss[a]

[a]*Department of Molecular Cell Biology, Max Planck Institute of Biophysical Chemistry, Am Fassberg, D-37077 Göttingen, Germany*
[b]*Departamento de Immunologia y Oncologia, Centro National de Biotecnologia, Universidad Autonoma Cantoblanco, E-28049 Madrid, Spain*
[c]*Laboratorio de Biologia del Desarollo Facultad de Ciencias, Universidad de Chile, Casilla 653, Santiago, Chile*
[d]*Centro de Biologia Molecular Severo Oatoa, C.S.I.C. and U.A.M., E-28049 Madrid, Spain*

Received 25 August 1997; revised version received 6 October 1997; accepted 7 October 1997

Abstract

In *Drosophila* the decision processes between the neural and epidermal fate for equipotent ectodermal cells depend on the activity of proneural genes. Members of the *Drosophila Iroquois-Complex* (Iro-C) positively regulate the activity of certain proneural *AS-C* genes during the formation of external sensory organs. We have identified and characterized three mouse *Iroquois*-related genes: *Irx1*, *-2* and *-3*, which have a homeodomain very similar to that of the *Drosophila Iro-C* genes. The sequence similarity implies that these three genes represent a separate homeobox family. All three genes are expressed with distinct spatio/temporal patterns during early mouse embryogenesis. These patterns implicate them in a number of embryonic developmental processes: the A/P and D/V patterning of specific regions of the central nervous system (CNS), and regionalization of the otic vesicle, branchial epithelium and limbs. © 1997 Elsevier Science Ireland Ltd.

Keywords: Iroquois; Prepattern gene; Homeobox; Mouse; Xenopus; Human; Neurogenesis; Otic vesicle; Branchial cleft; Limb

1. Introduction

During development of the mammalian nervous system, neuronal precursor cells within the ventricular zone proliferate and differentiate into the different cell types of neurons and glia. At the molecular level, however, little is known about the genes which direct neural cell commitment.

In *Drosophila*, genes playing critical roles during neural cell lineage determination have been identified, composing a network of proteins encoded by proneural and neurogenic genes, for reviews see (Campuzano and Modolell, 1992; Ghysen et al., 1993). Proneural genes, such as the four members of the *achaete-scute* complex (*AS-C*), mediate the delineation of groups of ectodermal equivalent cells (proneural cluster) and confer them the capacity to become neural precursors, reviewed by (Jan and Jan, 1994). Within a proneural cluster not all cells generate neurons, and this selection process requires a lateral inhibitory signaling mediated by the neurogenic genes. The key neurogenic genes such as *Delta*, *Notch*, *Suppressor of Hairless* [*Su(H)*], and the *Enhancer of split* complex [*E(Spl)-C*] encode proteins that restrict the adoption of a neural fate to one or a few cells within the proneural cluster, reviewed by (Muskavitch, 1994; Parks et al., 1997).

Homologs of the *Drosophila* proneural genes have been identified in many vertebrate species, and for some of them proneural activities have been reported (Allende and Weinberg, 1994; Ferreiro et al., 1994; Guillemot, 1995); for reviews see (Kageyama et al., 1995; Lee, 1997). An example of this is *Mash1*, which represents a mouse homolog of the *AS-C* genes, with an essential role during the formation of autonomic and olfactory neurons (Guillemot and Joyner, 1993; Sommer et al., 1995). In vertebrates, increasing evidence emphasizes the function of the neurogenic and proneural regulatory network to select individual cells from equivalent groups for specific fates (Bellefroid et al., 1997; Gómez-Skarmeta et al., 1997). The identification of

* Corresponding author.

0925-4773/97/$17.00
PII S0925-4773(97)00165-2

genes like *Hes* and *Id* representing the murine counterparts of *Hairy* and *emc*, two negative regulators of *A/S-C* genes, as well as the isolation of mammalian neurogenic genes supports this (Moscoso del Prado and Garcia-Bellido, 1984; Chitnis and Kintner, 1996).

In order to examine whether the evolutionary conservation of the proneural genes also includes some of their positive upstream regulators we focused on the *Drosophila* prepattern genes of the *Iroquois complex* (*Iro-C*). Two of these homeobox genes *araucan* (*ara*) and *caupolican* (*caup*), were recently reported to positively control the site specific activity of *ac* and *sc* (two genes of the *AS-C*) in sensory organ proneural clusters (Gómez-Skarmeta and Modolell, 1996; Leyns et al., 1996). Several lines of evidence indicate that the members of the *Iro-C* are required for the initial activation of *ac* and *sc* in certain sensory organ proneural clusters. In loss-of-function *Iro-C* mutants the lateral sensory organs on the notum of the flies fail to form, accompanied by a loss of *ac* and *sc* gene expression (Gómez-Skarmeta and Modolell, 1996; Leyns et al., 1996) and reviewed by (Vervoort et al., 1997). Furthermore, there is molecular evidence to show that Iro proteins are able to bind *A/S-C* enhancer sequences and that this binding is necessary for *ac* and *sc* expression (Gómez-Skarmeta and Modolell, 1996). Recent data imply the identification of a further member of the *Drosophila Iroquois* family: mirror (mrr), another homeodomain protein which is very similar to ara and caup, exhibits defined activity during eye development (McNeill et al., 1997).

The evolutionary conservation of at least some members of the genetic regulatory hierarchy that establishes neural fate during embryonic development encouraged us to screen for vertebrate *Iroquois* homologs.

In this study we present three members of the mouse *Iroquois* (*Irx*) gene family, referred to as *Irx1*, *-2* and *-3*. They share 92–95% amino acid identity in the homeodomain with the *Drosophila Iro-C* genes. All three genes are not only expressed in overlapping patterns, but also in specific patterns within the developing nervous system. The sequence conservation between Irx1, -2 and -3 to the *Drosophila* Iro proteins and their gene expression patterns during embryogenesis indicate that Irx1, -2 and -3 might be involved in early determination processes during nervous system development. This finding suggests the possibility that the neurogenic pathway appears to be conserved in species which are very distantly related, such as the fruitfly and the mouse.

2. Results

2.1. Characterization of the mouse Iroquois gene family related to the Drosophila Iro-C

We isolated three novel mouse genes from a mouse cDNA library using a *Drosophila ara* homeobox probe and low stringent hybridization conditions. The cDNA sequence analysis confirmed that three members of the mouse *Iroquois* homeobox family were cloned, which we named *Iroquois-homeobox-l*, *-2* and *-3* (*Irx1*, *-2* and *-3*) (Fig. 1A).

Alignments of the deduced homeodomains and flanking sequences of Irx1, -2 and -3 show regions of high amino acid sequence identity (82–92%) restricted mainly to the homodomains (Fig. 1B) and to some amino acids (up to 20) in the carboxy-flanking region (not shown).

Close inspection of the mouse Irx amino acid sequences revealed conservation of several features in addition to their homeodomains: the occurrence of potential phosphorylation sites for mitogen-activated protein kinase (MAPK) and some acidic regions downstream of the homeodomain. Such acidic regions may be involved in DNA-binding which has already been shown for flanking regions of other homeodomain proteins. Furthermore, a nine amino acid motif in the C-terminal portion without a known function was found to be conserved between Irx3 and Irx1 and ara, caup and mirror (not shown). This motif has not been found yet in Irx2, but it may be present in uncharacterized parts of the cDNA.

The highest degree of amino acid similarity among the different mouse homeodomain sequences was observed between Irx3 and Irx1 (Fig. 1A,B).

The amino acid sequences of the three murine Irx homeodomains have 92–95% identity with *Drosophila* ara, caup and mrr (Fig. 1B). This strongly supports the idea that the isolated mouse homeobox genes represent the mouse homologs of the *Drosophila Iro-C* genes. A Lysine at position 22 of the fly homeodomains represents a unique difference compared with vertebrate Iroquois homeodomains (Fig. 1A). The homeodomain of one of the three so far isolated *Xenopus* homologs of *Iroquois*-like genes, *Xiro3* (Bellefroid et al., 1997) has 100% similarity to the homeodomain of *Irx3*. Additionally, the 5' regions of Irx3 and Xiro3 have high sequence similarity. However the homeodomain of Irx1 and Irx2 show only 84 and 87% identity, respectively, to that of Xiro3. The homeodomains of the *Xenopus* Iroquois-like proteins Xiro1 and Xiro2 differ only in one amino acid from the murine homeodomains of Irx1 and Irx2, respectively (Gómez-Skarmeta et al., 1997).

The mouse Irx homeodomains have significant similarity (90–100%) to seven human EST (*e*xpressed *s*equence *t*agged) sequences available in the ATCC-database (Fig. 1A,B). These human Iroquois-like sequences also show a significant similarity (90–98%) to each other. One of the seven human Iroquois-like sequences (IRX1) has the same homeodomain amino acid sequence as Irx1 and Irx3, and the *Xenopus* Iroquois-like gene Xiro3. However, flanking regions of the homeodomain of this human IRX1 sequence differs more to that of Irx1 and Irx2 than to Irx3.

An alanine residue at position nine of the recognition helix (position 50 of the homeodomain) is characteristic for all members of the Iroquois protein family. No other

```
                                     I               II              III+IV
                               -------------    -----------    ------------------
                     1                                                  *      60
(D) Ara     YGASYDLAARRKNATRESTATLKAWLNEHKKNPYPTKGEKIMLAIITKMTLTQVSTWFANARRRLKKENKMTWEPKNR
(D) Caup    YGPNYDLAARRKNATRESTATLKAWLSEHKKNPYPTKGEKIMLAIITKMTLTQVSTWFANARRRLKKENKMTWEPKNK
(D) Mrr     SYGMDLNGARRKNATRETTSTLKAWLNEHKKNPYRTKGEKIMLAIITKMTLTQVSTWFANARRRLKKENKMTWEPRNR
(M) Irx1    YDG----PGRPKNATRESTSTLKAWLNEHRKNPYPTKGEKIMLAIITKMTLTQVSTWFANARRRLKKENKVTWGARSK
(M) Irx2    YPYQLNDPAYRKNATRDATATLKAWLNEHRKNPYPTKGEKIMLAIITKMTLTQVSTWFANARRRLKKENKMTWAPREQ
(M) Irx3    FGD----PSRPKNATRESTSTLKAWLNEHRKNPYPTKGEKIMLAIITKMTLTQVSTWFANARRRLKKENKMTWAPRSR
(H) IRX1    FGD----PSRPKNATRESTSTLKAWLNEHRKNPYPTKGEKIMLAIITKMTLTQVST
(H) IRX5    YGD----PGRPKNATRENTSTLKAWLNEHRKNPYPTKGEKIMLAIITKMTLTQVST
(H) IRX2b   YGD----PAYRKNATRDATATLKAWLNEHRKNPYPTKGEKIMLAIITKMTLTQVSTWFANARRRLKKENKMTWTRRNR
(H) Irx3    GAVELSGAGRRKNATRETTSTLKAWLNEHRKNPYPTKGEKIMLAIITKMTLTQVST
(H) IRX4    RYGTMDSGTRRKNATRETTSTLKAWLQEHRKNPYPTKGEKIMLAITTKMTLTQVST
(H) IRX2a   YGD----PAYRKNATRDATAILKAWLNEHRKNPYPTKGEKIMLAIITKMTLTQVSTWFANARRRLKKENKMTWTPRNR
(H) IRX6    YGD----PADRKNATRDATATXKAWLNEHRKNPYXTKGEKIMVAIITKMTLTQVSXW
```

	ara	caup	mirr	Irx1	Irx2	Irx3	IRX1	IRX2a	IRX2b	IRX3	IRX4	IRX5	IRX6
ara		98,4	86.7	95.0	95.0	95.0	95.0	91.7	93.4	95.0	93.4	93.4	91.7
caup			95.0	93.4	93.4	93.4	93.4	90.0	91.7	93.4	95.0	91.7	93.4
mirr				95.0	91.7	95.0	95.0	90.0	91.7	98.4	96.7	95.0	90.0
Irx1					91.7	100	100	90.0	91.7	96.7	95.0	98.4	90.0
Irx2						91.7	91.7	98.4	100	93.4	91.7	91.7	96.7
Irx3							100.0	90.0	91.7	96.7	95.0	98.4	90.0
IRX1								90.0	91.7	96.7	95.0	98.4	90.0
IRX2a									98.4	91.7	90.0	90.0	95.0
IRX2b										93.4	90.0	91.7	96.7
IRX3											98.4	96.7	91.7
IRX4												95.0	90.0
IRX5													90.0
IRX6													

(dark)	95.0-100%
(grey)	90.0-94.9%
(white)	-89.9%

Fig. 1. (A) Comparison of the putative Irx1, -2 and -3 homeodomain sequences with other Iroquois-related homeodomain sequences. Bold represents amino acid identity throughout the whole Iroquois family. Capital letters in parentheses denote the following: D, *Drosophila* (Gómez-Skarmeta and Modolell, 1996; McNeill et al., 1997); M, mouse (EMBL Nucleotide Sequence Database accession numbers for *Irx1, -2* and *-3* genes are: Y15002, Y15001 and Y15000, respectively); H. human. The amino acids are numbered, starting at 1 from the first amino acid of the homeodomain. Roman numbers on top represent the helices of the homeodomain. The *Iroquois* family of homeobox genes encodes proteins characterized by the presence of an alanine residue at position 50 of the homeodomain. *Irx1, Irx3*, and five of seven human sequences lack four amino acids in front of the homeodomain, in comparison with *Drosophila* and the remaining two human sequences. Sequence inconsistencies within the homeodomain of the human IRX6 derived from the database are depicted as an X. (B) Pairwise comparisons of percentage amino acid identity in the conserved homeodomains among *Drosophila*, mouse and human Iroquois family members. We assumed the not determinable amino acids (X) in IRX6 as conserved in comparison with the other *Iroquois* homeodomains.

known homeodomain has an alanine at this specific position. This alanine residue is placed in the major groove of the homeodomain and it is a major determinant of DNA-binding specificity (Treisman et al., 1989).

Taken together, the structural similarities between the mouse, *Drosophila*, *Xenopus* and human *Iroquois*-like genes suggest that they constitute members of a new family of homeobox containing genes.

2.2. Detection of Irx1, -2 and -3 transcripts by Northern blot analysis

Northern blots with total and polyA$^+$ RNA samples isolated from E10.5–E17.5 mouse embryos were used to determine the sizes of *Irx1, -2* and *-3* transcripts.

The *Irx1* probe identified a 2.5 kb transcript (Fig. 2A). The *Irx2* probe detected two distinct transcripts of 2.1 and 2.9 kb, respectively, (Fig. 2B). The *Irx3* probe detected two transcripts of 2.3 and 2.8 kb, respectively, (Fig. 2C). These data confirmed that the different cDNAs correspond to three different genes.

2.3. In situ analysis of Irx1, -2 and -3 expression during early embryogenesis (E6.5–E7.5)

We compared the expression of the mouse *Irx1, -2* and *-3*

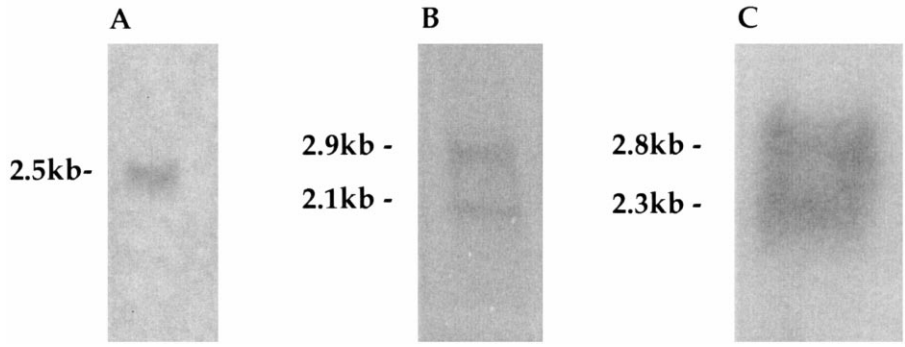

Fig. 2. Northern blot analysis of *Irx1*, *-2* and *-3* in post-implantation embryos. The size of the transcripts are indicated on the left and were estimated by comparison with the RNA ladder from Boehringer (not shown). The lane (A) represents a Northern blot of 10 μg total RNA isolated from E14 and hybridized with a 400 bp *Irx1* specific probe excluding the homeobox. Only one band was visible after hybridization with *Irx1* corresponding to a molecular weight of 2.5 kb. (B) The *Irx2* probe (1.4 kb) encoding parts of the homeobox and adjacent sequences detected two transcripts of 2.1 and 2.9 kb. (C) Three micrograms of polyA$^+$ RNA from E14.5 was hybridized with a 1.1 kb *Irx3* probe comprising the 3′ region of the homeobox and adjacent sequences. This *Irx3* probe detects two bands of 2.3 and 2.8 kb. The size differences between the transcripts and the cDNA fragments indicate that the *Irx1* and *Irx2* cDNAs are incomplete at their 5′ ends.

genes during embryonic development between E6.5 and E10.5 by whole mount in situ hybridization.

Irx3 is the earliest of the *Iroquois*-family genes to be expressed. Transcripts of *Irx3* are first found at E6.5 in the extraembryonic portion of the egg cylinder, at high levels in the ectoplacental cone and in the lining of the ectoplacental cavity (data not shown). All the structures expressing *Irx3* are trophectoderm derivatives. The chorionic ectoderm which develops from the ectoplacental cone also shows *Irx3* transcripts at mid-gastrulation (Fig. 3C).

The embryonic expression of *Irx3* starts at E7.5 as two symmetrical patches in the anterior region of the embryo (Fig. 3C). At the same time the first *Irx1* expression is seen in comparable regions of the embryo (Fig. 3A). Transverse sections revealed that *Irx1* transcripts are restricted to the mesodermal wings overlying the presumptive head-fold region (Fig. 3D). In contrast, *Irx3* signals are confined to the ectodermal layer where they represent two expression domains in the margins of the neural plate (Fig. 3F). *Irx2* expression is not yet detectable at these stages (Fig. 3B).

2.3.1. All three Irx genes display distinct expression patterns during neural tube closure

At E8.5, *Irx3* mRNA is found dorsolaterally in the neural folds of the prospective mesencephalon, within the rhombencephalon mostly in the precursor regions of rhombomere 1 and -3, and additionally in the rostral part of the closing neural plate (Fig. 3I,L). During the ongoing development, *Irx3* signals extend further towards the caudal region of the

Fig. 3. Expression of mouse *Irx* genes at mid-gastrulation stage E7 5 up to early neurulation at E8.5 (10–12 somites). Anterior is to the left. (A,B,C) lateral views on E7.5 embryos. (A) shows expression of *Irx1* only in the embryonic portion. (C) shows *Irx3* expression in extraembryonic and embryonic parts of the egg cylinder. At this stage, no transcripts of *Irx2* are detectable (B). (D,F) transversal sections of the E7.5 embryos in (A,C). The plane of sections are illustrated (E). (F) *Irx3* expression within the E7.5 embryo is confined to the ectodermal layer. (D) expression of *Irx1* is restricted to the mesodermal wings. Expression of *Irx* genes in E8.5 embryos (G–L). (I,G) lateral and (H) dorsolateral views of E8.5 embryos. (G) shows expression of *Irx1* in the presumptive midbrain and in the anterior foregut. Initial pre-rhombolnere 4 (pre-r 4) specific expression of *Irx2* is seen in (H). The rhombomere identification was possible in respect to the preotic sulcus. (I) represents *Irx3* expression in the presumptive midbrain, hindbrain and in the anterior spinal cord as well as in the anterior foregut. (L) transverse section at the hindbrain level of the embryo in (I) revealing the *Irx3* expression in the neuroepithelium of the presumptive hindbrain as well as in the epithelium of the branchial pouches. (J) saggital section of the embryo in (G) which reveals the *Irx1* transcripts in the presumptive hindbrain and in the posterior spinal cord where it is already closed. In (J), the contour of the embryo has been partially delineated to make the identification of the labeled regions easier. (K) transverse section at the hindbrain level of a slightly older (E8.75) embryo than the one in (H) with *Irx2* expression limited to the neuroepithelium of the presumptive hindbrain at the level of pre-r 4. FB, forebrain; bpo, branchial pouches; ect, embryonic ectoderm; exe, extraembryonic ectoderrn; FG, foregut; H. heart; HB, hindbrain; MB, midbrain; mes, mesoderm; pos, preotic sulcus; rh4, rhombomere 4; SP, spinal cord.

Fig. 4. Overview of the *Irx* expression profiles at E9.5 (A,B,C) and E10.5 (D,E,F) embryos. The embryo in (A) was hybridized with *Irx1* showing expression in the midbrain, hindbrain, epithelium of the first and second branchial arches and foregut. (B) depicts an embryo with *Irx2* expression in the midbrain, hindbrain, spinal cord, epithelium of the first and second branchial arches and foregut. (C) shows *Irx3* expression in the midbrain, hindbrain, entire spinal cord, epithelium of the first and second branchial arches, cephalic mesenchyme, lateral plate mesenchyme and foregut. At E10.5 mid-gestation stage, (F) the *Irx3* expression extends within the posterior forbrain up to the hypothalamic region (arrowhead in F). *Irx1* and *Irx2* have their rostral limit of expression in dorsalthalamic regions (D,E). The cephalic mesenchyme expression domain of *Irx3* at E10.5 includes the nasal pits (F). Weak expression of *Irx1* and *Irx2* within the developing limb starts at E10.5: (D) *Irx1* in the region were the AER arises and (E) *Irx2* in the dorsal part. FG, foregut; bare, epithelium of the branchial arch; cem, cephalic mesenchyme; HB, hindbrain; lpm, lateral plate mesoderm; MB, midbrain; HB, hindbrain; PT, pretectum; som, somite; SP, spinal cord.

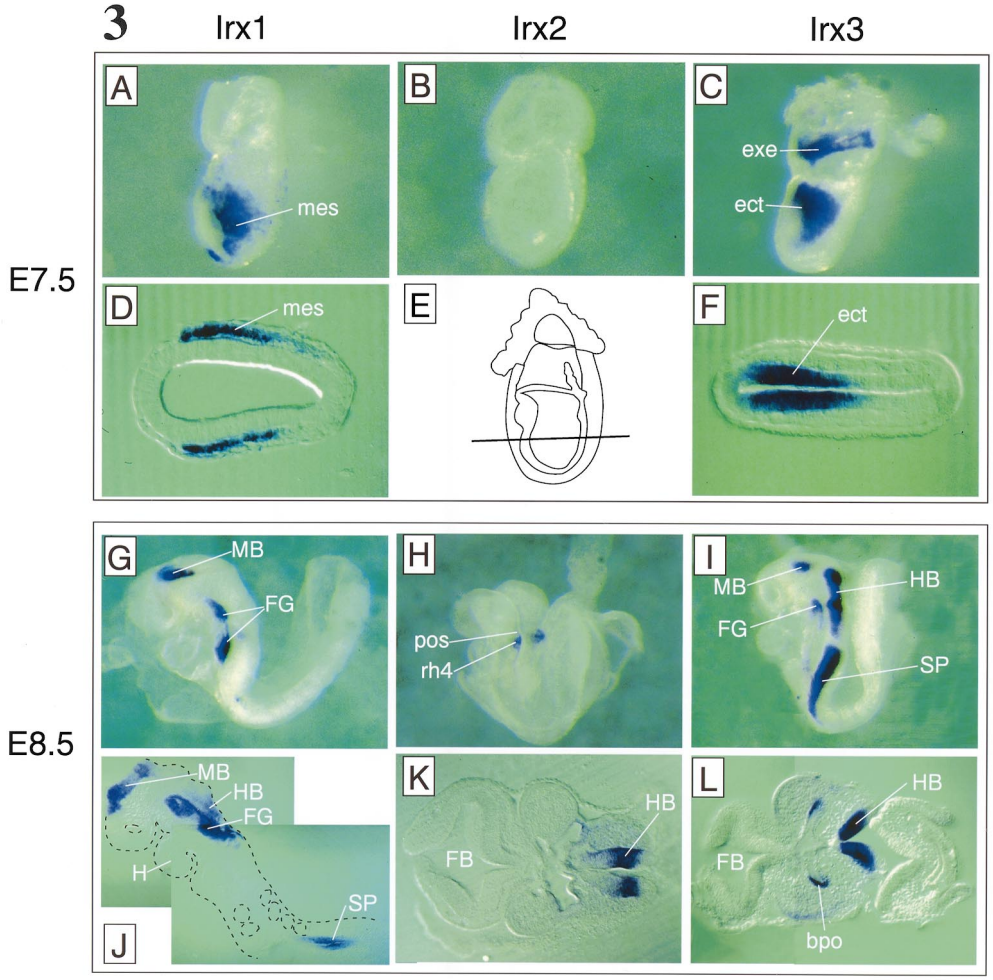
3
Irx1
Irx2
Irx3
E7.5
A
mes
B
C
exe
ect
D
mes
E
F
ect
E8.5
G
MB
FG
H
pos
rh4
I
MB
HB
FG
SP
J
MB
HB
FG
H
SP
K
HB
FB
L
HB
FB
bpo

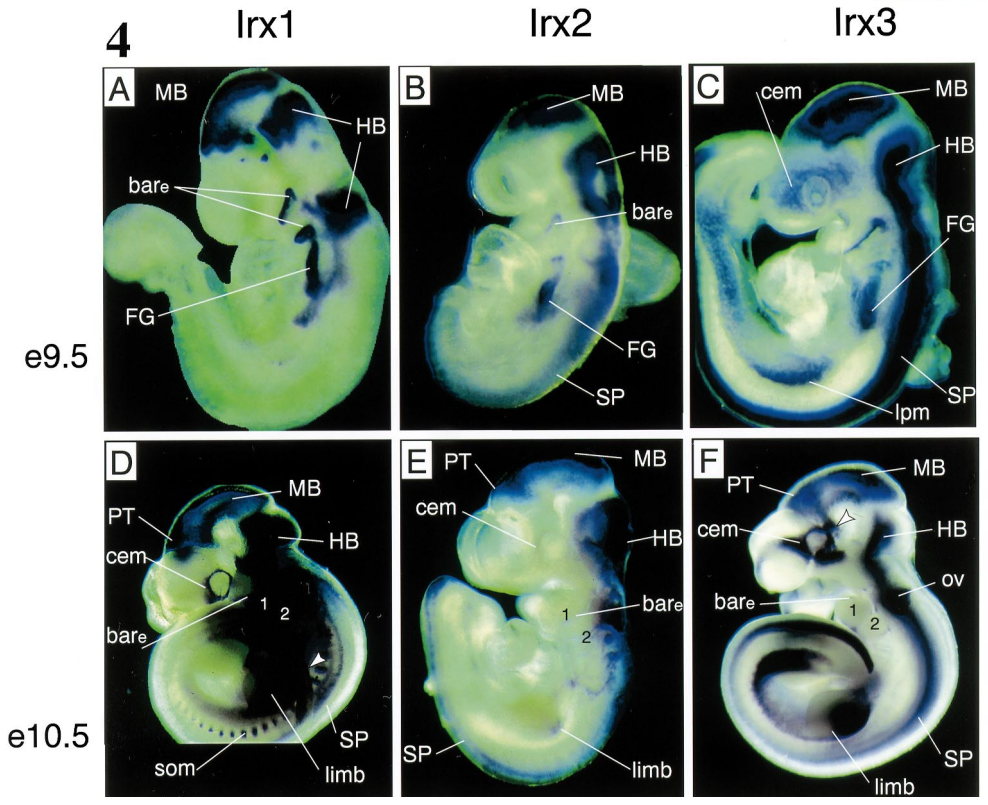
4
Irx1
Irx2
Irx3
e9.5
A
MB
HB
bare
FG
B
MB
HB
bare
FG
SP
C
cem
MB
HB
FG
SP
lpm
e10.5
D
MB
PT
HB
cem
bare
1
2
SP
som
limb
E
PT
MB
cem
HB
bare
1
2
SP
limb
F
PT
MB
cem
HB
ov
bare
1
2
SP
limb

neural tube. Within the neural tube, *Irx3* transcripts are confined to the ventricular site (close to the lumen) of the alar plate, excluding the roof plate and the most dorsal region (Fig. 7C).

Irx1 and *Irx2* transcript distributions within the developing nervous system appear more restricted in comparison to *Irx3*. The most prominent expression of *Irx1* in the brain is confined to the dorsolateral walls of the mesencephalon (Fig. 3G). Sagittal sections also revealed a weak expression in the rhombencephalon and within the posterior region of the neural tube (Fig. 3J). At this stage, *Irx2* expression appears for the first time in the rhombencephalon, specifically active in the presumptive region of future rhombomere 4 (Fig. 3H).

2.3.2. During neurogenesis (E9.5–E10.5) Irx1, -2 and -3 are predominantly expressed along the anteroposterior axis of the CNS

At E9.5 all three *Irx* genes display restricted patterns of expression along the A/P axis of the developing neural tube with a common rostral limit at the level of the pretectum (Fig. 4A,B,C). All *Irx* genes are strongly expressed in the tectum of the mesencephalon, whereas in the tegmentum only *Irx3* and *Irx1* transcripts are found (Fig. 4A,B,C). The hindbrain also exhibits A/P-specific expression of the three *Irx* genes: *Irx3* is expressed throughout the entire hindbrain while *Irx1* and *Irx2* are restricted to specific rhombomeres (Fig. 4A,B,C). Sagittal sections reveal only a faint appearance of *Irx1* mRNA within the dorsal portions of the rhombomeres 2, 3 and 4 (Fig. 7B). At this stage *Irx2* expression is found in rhombomeres 1–4 and 7–8 (Fig. 4B). It is worth noting that the border region between mesencephalon and rhombencephalon and the anterior prosencephalon do not show any *Irx* gene activity.

In the rostral spinal cord, *Irx3* transcripts are found in the alar and basal plate, but not in the roof- and floorplate (Fig. 5I,L). In caudal regions of the spinal cord *Irx3* is expressed only in the alar plate (Fig. 5L). In contrast, *Irx2* expression in the spinal cord is much weaker and confined to the alar plate along the entire spinal cord (Fig. 5H,K). The expression of *Irx1* is only observed in the spinal cord posterior to the region of the developing hindlimb (Fig. 5J).

At E10.5, the expression domains of all *Irx* genes extend rostrally into the dorsal diencephalon, while the characteristic patterns of their early expression are maintained (Fig. 4D,E,F). The rostral boundary of *Irx1* and *Irx2* expression extends to the presumptive domain of the zona limitans intrathalamica (Fig. 4D,E). Only *Irx3* shows expression in the basal plate of the diencephalon (arrowhead in Fig. 4F). Furthermore, *Irx3* expression in the mesencephalic roof exhibits a posterior-to-anterior gradient (Fig. 4F).

Additionally, in the spinal cord *Irx3* transcripts are localized in cells of the ventricular layer and in the motoneuron column of the basal plate (Fig. 7E). The alar plate reveals also two restricted areas in the marginal layer.

In these stages, *Irx1* expression extends into the entire ventral spinal cord, but the strongest expression remains in the most caudal region (arrowhead in F. 4D). From this time onwards *Irx1* expression domain is restricted to the ventral spinal cord.

2.3.3. Complementary expression of Irx1, -2 and -3 during early development of the inner ear

Starting at the otic vesicle stage, there is a remarkable regionalized expression pattern of all three *Irx* genes in the developing inner ear (Fig. 6). Transverse sections of E9.5 embryos at the level of the hindbrain reveal the expression of *Irx1* within the lateral wall of the otic vesicle (Fig. 6A). This region partially overlaps with the *Irx2* expression domain in the lateroventral part of the otic vesicle (Fig. 6A,B). In contrast to *Irx1* and *Irx2*, the distribution of *Irx3* transcripts is restricted to the ventromedial portion of the otic vesicle adjacent to the hindbrain (Fig. 6A,B,C). The dorsal region of the otic vesicle is devoid of any detectable *Irx* transcripts. From E10.5 onwards, all three *Irx* genes are expressed in the entire otic vesicle.

The condensing mesenchyme on the ventral side of the otic vesicle also displays expression of *Irx1*, *-2* and *-3* (arrowhead in Fig. 6). The surrounding mesenchyme is necessary for proper spatial development of the vestibular and auditory receptors, and for the formation of the cartilages which later surrounds the inner ear (Ruben et al., 1986).

2.3.4. Specific expression of Irx1, -2 and -3 during limb development

Only *Irx3* is expressed in the prospective limb territories

Fig. 5. Vibratome transverse sections of embryos at E9.5 following *Irx* whole mount in situ hybridization. (A–F) *Irx1*, *-2* and *-3* expression in the hindbrain. *Irx* gene expression in the cephalic mesenchyme around the eye (F) and in cells which may participate in the trigeminal ganglia formation (A,F). *Irx1*, *-2* and *-3* are transcriptionally active in the foregut (G–I), in particular in regions which develop the lungbud (tracheal diverticulum) (J–L). *Irx1* expression within the spinal cord is restricted to a caudal region (G,J). Weak *Irx2* expression within the spinal cord is restricted to the alar plate (H). (I,L) shows *Irx3* expression in the entire spinal cord. *Irx1* (D,G) and *Irx2* (B,E,H,K) are transcriptionally active in the surface ectoderm. FB, forebrain; bpo, branchial pouches; cem, cephalic mesenchyme; ect, surface ectoderm; FG, foregut; HB, hindbrain; lpm, lateral plate mesoderm; MG, midgut; SP, spinal cord; tra, tracheal diverticulum.

Fig. 6. Regionalized *Irx* expression in the otic vesicle. Whole mount in situ hybridization of transverse sections (A,B,C) at the hindbrain level of the E9.5 embryos in (D,E) which are depicted in dorsal views. *Irx1* (A) and *Irx2* (B) overlap in lateroventral regions; *Irx1* expression extends further laterally than *Irx2*. (C) *Irx3* expression is restricted to the otic vesicle neuroepithelium adjacent to the hindbrain. HB, hindbrain; ov, otic vesicle.

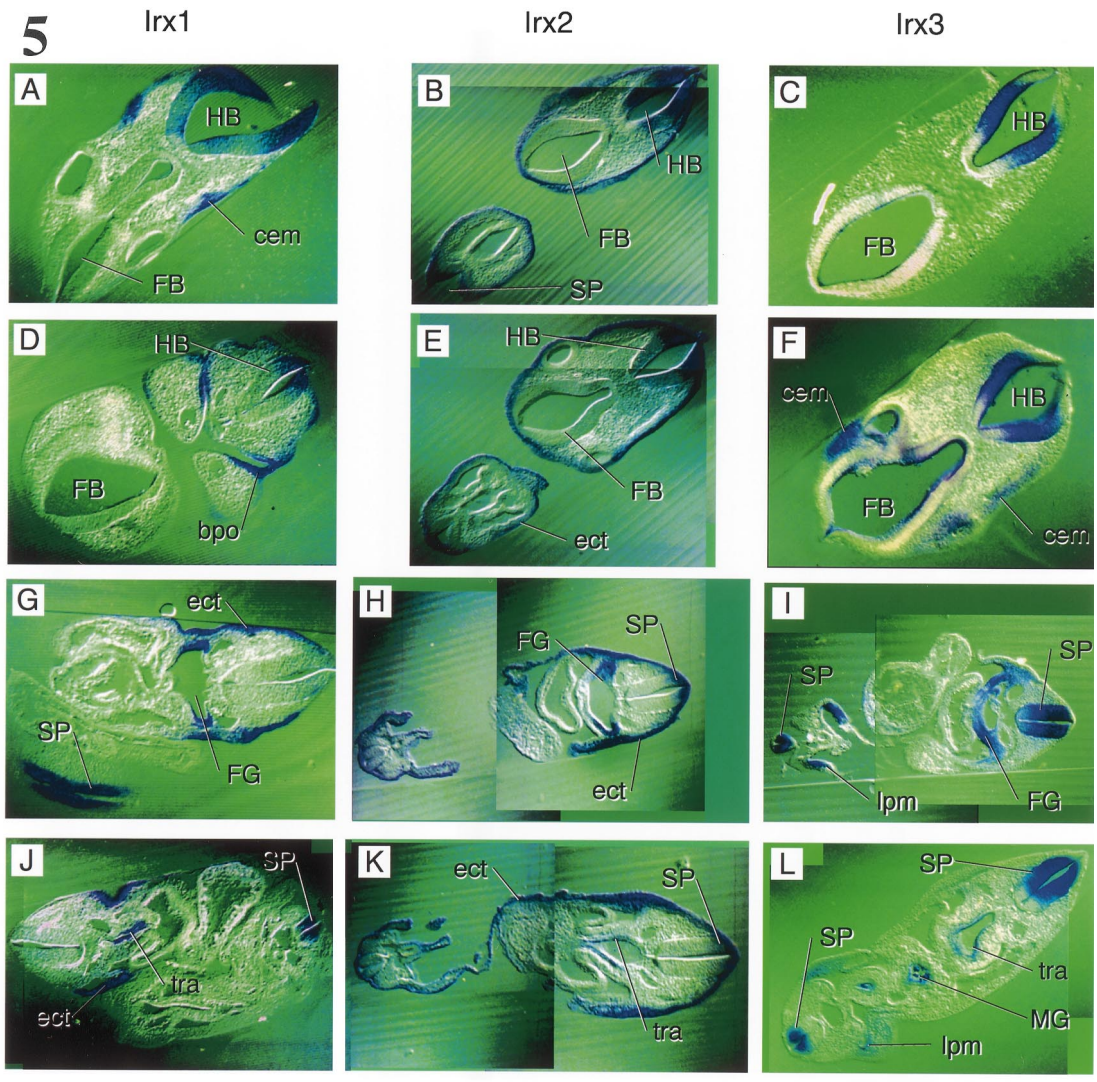
5
Irx1
Irx2
Irx3
A
HB
cem
FB
B
HB
FB
SP
C
HB
FB
D
HB
FB
bpo
E
HB
FB
ect
F
cem
HB
FB
cem
G
ect
SP
FG
H
FG
SP
ect
I
SP
SP
lpm
FG
J
SP
tra
ect
K
ect
SP
tra
L
SP
SP
tra
MG
lpm

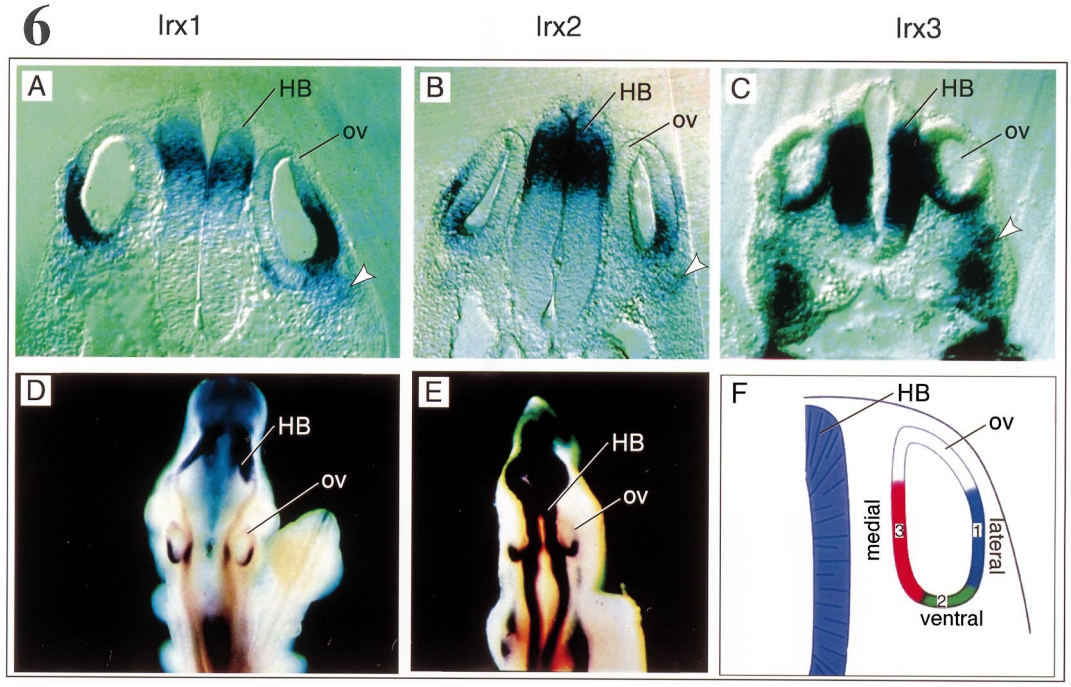
6
Irx1
Irx2
Irx3
A
HB
ov
B
HB
ov
C
HB
ov
D
HB
ov
E
HB
ov
F
HB
ov
medial
lateral
ventral
3
1
2

of the lateral plate mesoderm from E9.0 onwards (Fig. 4C). From E10.5 onwards, the *Irx* genes exert distinct patterns of expression in the developing limb buds (Fig. 4D,E,F). Transcripts of *Irx3* exhibit a gradient of expression along the dorsoventral and the proximodistal axes with their highest level in the proximodorsal margin of the limb (Fig. 7D). This expression extends distally as the limb grows and maintains the gradient. From E10.5 onwards *Irx1* and *Irx2* start to be expressed in the limb bud (Fig. 4D,E). *Irx1* appears to be very faintly expressed in a region where the apical ectodermal ridge (AER) arises (Fig. 4D). Only a weak *Irx2* expression is detectable in

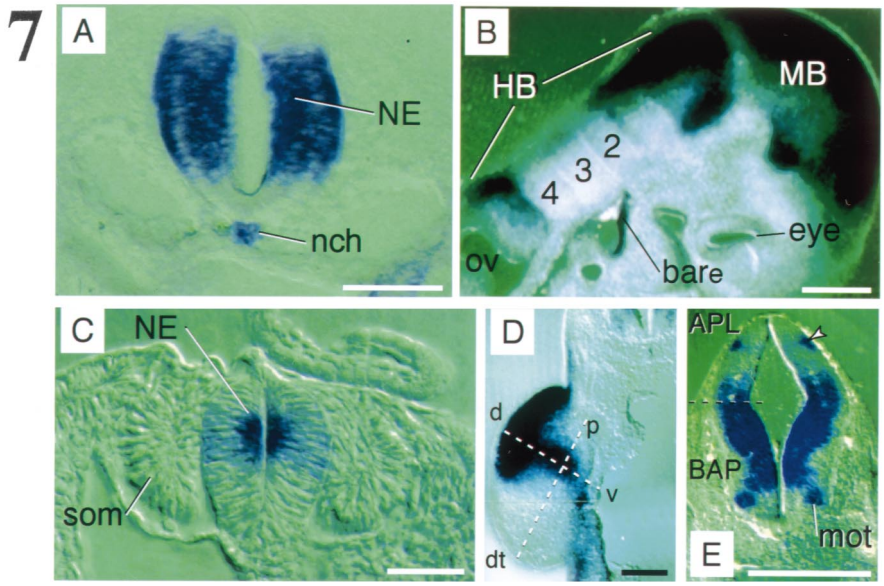

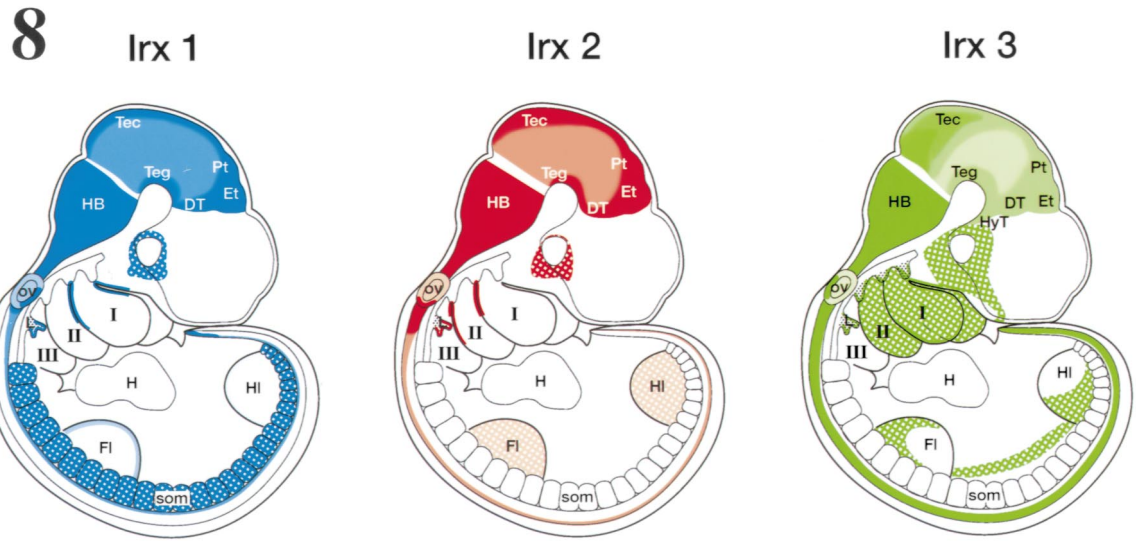

Fig. 7. Special aspects of *Irx* expression. (A) Transverse section of an E9.0 embryo showing *Irx3* expression in the notochord and neural tube. (B) Midsagittal section of an E9.5 embryo with *Irx1* expression restricted to dorsal portions of the rhombomeres 2, -3 and -4, the midbrain and the ectodermal layer of the first branchial arch. (C) Transverse section of an E8.5 embryo shows *Irx3* positive ventricular cells close to the lumen of the neural tube. (D) Section of a limb at E10.5 with *Irx3* transcript accumulation in proximodorsal regions. (E) Transverse section of an E10.5 spinal cord showing *Irx3* labeling in the ventricular layer and in the motoneuron columns of the basal plate. Arrowhead marks the *Irx3* expressing cells in the marginal layer of the alar plate. Scale bars represent ~50 μm in (A,C) and ~250 μm in (B,D,E). APL, alar plate; BAP, basal plate; bare, epithelium of the branchial arch; d, dorsal; dt, distal; H. heart; HB, hindbrain; Hl, hindlimb; MB, midbrain; mot, motoneuron; nch, notochord; NE, neuroepithelium; ov, otic vesicle; p, proximal; som, somites; v, ventral.

Fig. 8. Schematic summary of the comparative expression analysis of *Irx1*, *-2* and *-3* between E9.5 and E10.5. Hatched areas delineate mesodermal derivatives. Endodermal derivatives are depicted with black dots. *Irx* expression within the CNS is shown colored. The three genes are expressed along the CNS with a rostral limit at the dorsal thalamus except for *Irx3* which extends to the hypothalamus. I–IV, branchial arches I–IV; DT, dorsalthalamus; ET, epithalamus; Fl, forelimb;; H. heart; HB, hindbrain; Hl, hindlimb; Hyt, hypothalamus; L, lungbud; MB, midbrain; PT, pretectum; som, somites; VT, ventralthalamus.

the dorsal portion of the limb bud (Fig. 4E). At E11.5 transcripts of *Irx1* appear strongly in the forelimb digits (not shown).

2.3.5. Irx1, -2 and-3 expression in other tissues during early stages of organogenesis

Both *Irx1* and *Irx3* are expressed in two symmetrical patches in the embryonic mesodermal layer, with *Irx3* expression being very faint. They begin to express at stages E7.5 and E7.75, respectively (Fig. 3D). However, only *Irx3* is detected in the notochord at stage E9.0 (Fig. 7A). At E9.5 transcripts of *Irx1* and *Irx3* and later also of *Irx2* (at E10.5) are found in the cephalic mesenchyme around the optic vesicle which is involved in the formation of the outer layers of the eyes, the eye muscles and the lachrymal glands (Fig. 4A,C,E). Around E10.5, the *Irx3* signals in the head mesoderm extend into the nasal pits (Fig. 4F). Furthermore, all three genes are found in putative cephalic mesenchymal cells which in time may participate in trigeminal and fascio-acustic ganglia formation (Fig. 5A,F). At later stages the *Irx* genes are transcriptionally active in the V and VII–VIII cranial ganglia (not shown). The cranial ganglia are known to have two embryonic origins: the cephalic neural crest and the epibranchial placodes. From E9.5 onwards, the branchial clefts including the regions of the branchial placodes, reveal different restricted expression patterns of all three genes in distinct ectodermal regions between the mandibular, maxillar and hyoid swellings (Fig. 4 A–F), schematically summarized in Fig. 8. However, no *Irx* expression is detectable in migrating neural crest cells. Later on, the external ears (derivatives of the epibranchial placodes) show expression of *Irx1*, *-2* and *-3* (not shown).

Beginning with E9.5, *Irx1* and *Irx2* exhibit expression in the superficial ectoderm surrounding the body, with *Irx1* transcripts being restricted to the ectoderm at the level of the hindbrain (Fig. 5D,E,G,K).

From E8.5 onwards, *Irx1* and later all three *Irx* genes (E9.5) are expressed in the region of the foregut, which will form the pharynx and the lung bud (Fig. 3G). This expression domain is maintained at later stages in the epithelial layer of the bronchiae (Fig. 5).

At E10.5 only *Irx1* expression appears in the somites and becomes later restricted to the myotome (Fig. 4E and section not shown).

3. Discussion

We have characterized three mouse homeobox genes *Irx1*, *-2* and *-3* related to genes of the *Drosophila Iro-C* locus. These mouse genes code for proteins exhibiting a very high homeodomain sequence conservation as their *Drosophila* counterparts. Their expression precedes and overlaps the expression of distinct proneural genes in the mouse.

3.1. Conservation of the predicted protein sequences of the murine Iroquois-like genes is mainly restricted to their homeodomains

The primary protein sequences of Irx1, -2 and -3 reveal a high degree of identity (92–100%) within their homeodomains. This extreme amino acid sequence conservation in Iroquois-like proteins was also found when compared to such evolutionary distant species as *Drosophila*, *Xenopus* and human (up to 100% amino acid identity between mouse and human). An alanine residue at position 9 of the recognition helix is a characteristic feature for the Iroquois family of homeodomains. Due to the high sequence similarity and the characteristic expression patterns we consider the mouse *Iroquois*-like genes as a separate homeobox family as it was proposed by Gómez-Skarmeta and Modolell (1996). Preliminary data indicate that the murine *Iroquois*-like gene family is larger than the three members presented (unpublished observations).

3.2. Involvement of Irx genes during neurogenesis

The finding that *Drosophila Iro-C* members regulate proneural genes suggests that the murine *Irx* genes could play a similar role during mouse neurogenesis. In *Drosophila*, the genes of the *Iroquois*-complex are expressed in the head of the embryo, epidermis and in broad territories within the imaginal wing disc that include the proneural clusters which give rise to the sensory organ precursor cells (Gómez-Skarmeta and Modolell, 1996). However, the exact pattern of expression in the head of the fly embryo has not yet been described.

Three *Xenopus* homologs of the *Iroquois* family are found to be expressed in the neuroectoderm and anterior mesoderm, overlapping *Xash3* expression (Bellefroid et al., 1997; Gómez-Skarmeta et al., 1997). Their recent data imply that the *Iroquois*-like genes in *Xenopus* promote neurogenesis upstream of *Xash3* and other proneural genes.

The early and transient expression of the mouse *Irx* genes during initial stages of neural development represents a common feature of the vertebrate and invertebrate *Iroquois* family members. *Irx3* is expressed in the neuroectoderm at a time when the neural plate begins to form (E7.5). Whether this similarity in the chronology of gene activity indicates that this part of the network of interacting genes is also conserved through evolution remains to be investigated.

Furthermore, the localization of *Irx3* transcripts in the ventricular zone of the alar plate of the spinal cord containing uncommitted neural precursor cells suggests that *Irx3* could play a role in the development of sensory neurons.

Neurogenesis in mammals requires progressive regionalization along the A/P and D/V axes resulting in regions with distinct molecular traits. Many transcription factors and regulatory molecules participate in these patterning processes as shown for the *Hox*, *Pax*, *Nkx* and *POU* gene families (Guillemot, 1995). For example, evidence has

been presented for the involvement of *Hox* genes in the specification of hindbrain identities, for reviews see (McGinnis and Krumlauf, 1992; Keynes and Krumlauf, 1994). During vertebrate hindbrain development, 8 metameric units, termed rhombomeres, appear. Only a few genes are described which display a rhombomere specific activity such as *Hoxbl*, the most 3' member of the *HoxB* group and the zinc-finger transcription factor *Krox20* (Goddard et al., 1996); reviewed by (Lumsden and Krumlauf, 1996).

Interestingly, even prior to the formation of morphologically recognizable rhombomeric units, *Irx2* expression is restricted to the hindbrain neural ectoderm giving rise to pre-rhombomere 4 (pre-r4). *Irx3* signals accumulate in pre-r1 and pre-r3. These specific expression patterns suggest that the *Iroquois*-like genes may be involved in rhombomere territory delineation and could be useful markers for rhombomere identities.

At E9.5 all three *Irx* genes exhibit an anterior expression border at the pretectum. One day later, this border expands to the dorsal thalamus. Only *Irx3* extends its expression also into the basal plate of the diencephalon.

Within the mesencephalic roof *Irx3* exhibits a rostrocaudal gradient of expression. The earliest genes reported so far with expression in a gradient-like manner are the *Engrailed* genes, reviewed by (Lumsden and Krumlauf, 1996). Knockout experiments demonstrated that *Enl* is indeed involved in establishment of midbrain polarity, reviewed by (Joyner, 1996).

The *Irx* genes may also participate in the A/P regionalization of the spinal cord. While *Irx3* and *Irx2* were active along the entire A/P axis of the spinal cord at E9.5, transcripts of *Irx1* were limited to the region posterior to the hindlimb bud. One day later *Irx1* expression extends rostrally, but still exhibits its most intensive expression in the tail bud region.

Moreover, *Irx1*, *-2* and *-3* display distinct patterns also along the D/V axis of the developing CNS suggesting a possible involvement in early neuronal regionalization. *Irx3* is the only *Irx* gene with expression in the basal plate within the diencephalon, while both *Irx1* and *Irx2*, are limited to the dorsal and ventral thalamus, which are alar plate derivatives. Within the mesencephalon as well as the pretectum and tectum (the last two being alar plate descendants) all three *Irx* genes are expressed. The basal mesencephalic domain, the tegmentum, expresses *Irx3* and *Irx1*, but not *Irx2*. The spinal cord also displays a distinct D/V pattern of *Irx* genes: *Irx1* appears to be specific for ventral (basal) territory while *Irx3* and *Irx2* are restricted to the most dorsal region. It is remarkable that the main *Irx3* and *Irx2* expression domains in the neural tube occur in alar plate derivatives.

Candidates for determination of neuronal identities in the CNS are *Pax3*, *Pax7* and *Mash1* which are expressed during dorsal cell differentiation, and also *Pax6* and *Neurogenin* which are expressed in medial/ventral regions, for reviews see (Mansouri et al., 1996; Tanabe and Jessell, 1996).

In conclusion, the *Irx* genes may participate in the signaling cascade during the regionalization along the neuraxis. Their distinct spatio/temporal expression profile between E9.5 and E10.5 is schematically summarized in Fig. 8.

The overlap in expression patterns of the three *Irx* genes during early embryogenesis raises the possibility of functional redundancy of these genes. A systematic mutational analysis of single and compound mutants of the *Irx* genes, together with the comparative expression studies as presented here, will identify both the functions that are shared among the different members and the unique roles of each of them.

3.3. Complementary expression of the murine Irx genes in the otic vesicle suggests a role in pattern formation during inner ear development

The otic vesicle is formed by a process of condensation of ectodermal cells into the otic placode, which then invaginates into the mesenchyme lateral to rhombomere 5 and -6. The otic vesicle gives rise to the inner ear which is also described as the membranous labyrinth and contains the sensory organs for hearing and balance. Between E9 and E10, the otic vesicle becomes regionally determined, although its neuroepithelial walls still look homogenous (Ruben and Rapin, 1980; Swanson et al., 1990).

The expression patterns of otic vesicle regionalizing genes may indicate the future cell fate of the developing inner ear, for review see (Fekete, 1996; Rivolta, 1997). Inactivation of a few of these genes lead to inner ear malformations which help to determine the region of the otic vesicle which gives rise to the individual structures of the inner ear (Mansour et al., 1988; Torres et al., 1996; Hadrys et al., 1997). Firstly, the dorsomedial aspect of the otic vesicle extends to form the endolymphatic sac while its ventral end differentiates into the cochlea. The utricular region descending from lateral and dorsal parts differentiates to form the three semicircular canals. These differentiation processes during inner ear formation, as in any other organ system, most likely result from the temporal and spatial expression of a selected array of genes.

The complementary expression of the three *Irx* genes suggests that they together with other regulatory genes contribute to the development of inner ear components.

Specifically, the region of *Irx1* activity in the lateral portion of the otic vesicle overlaps with the expression of the homeobox gene *Nkx5.1*. Loss-of-function of *Nkx5.1* results in malformation of all three semicircular canals (Hadrys et al., 1997). Thus, one can speculate that *Irx1* also participates in semicircular canal formation *Irx2*, with its transcriptional activity in ventrolateral regions of the auditory vesicle, may be involved in cochlea development. *Irx3* signals were confined to the otic vesicle neuroepithelium adjacent to the hindbrain, similar to the expression of *Pax2*. Since mice

in loss-of-function studies of *Pax2* exhibited cochlea and ganglia defects (Torres et al., 1996) we suppose that *Irx3* also participates in cochlea development and formation of the VIII ganglion. Moreover, *Irx3* and *Pax2* may be functionally related because their expressions overlap completely at the onset of *Pax2* activity in late primitive streak stages (Rowitch and McMahon, 1995).

It is known that inductive processes mediated by rhombomere 5 and -6, which are required for the formation and subsequent development of the auditory and balance system in vertebrates (Wilkinson et al., 1988; Noden and Van de Water, 1992). *Fgf3* (*Int2*) whose expression occurs in a region proposed as an inductive area for the otic vesicle is presumed to encode a diffusible factor produced by the hindbrain (Wilkinson et al., 1989). In loss-of-function *Fgf3* mutants the otic vesicle and tail structures fail to develop properly (Mansour et al, 1988). However, in these mice the induction of the otic vesicle itself is not affected, rather, its subsequent development.

According to these observations it is of particular interest that all three *Irx* genes are strongly expressed in rhombomere 5 and -6 when the initiation of the otic placodes takes place, indicating a possible involvement of *Iroquois*-like genes in morphogenetic induction events during the formation of the otic vesicle (at about E8.0–E8.5).

During embryonic inner ear development our expression data imply two different involvements of the mouse *Irx* genes: firstly, during otic vesicle induction by the hindbrain, and secondly, during otic vesicle patterning and differentiation.

3.4. Specific Irx activity suggests roles in determination of limb territories

The limb bud emerges from thickened lateral plate mesoderm which condenses with its ectodermal covering. Members of the *Fgf* family are known to initiate limb bud outgrowth (Dealy et al., 1996; Ohuchi et al., 1997). *Irx3* activity at E9.0 in the lateral plate mesoderm (prior the limb bud appearance) suggests a role during these early limb formation processes.

The limb as an asymmetric structure is defined on three axes: anterioposterior (A/P), proximodistal (P/D) and dorsoventral (D/V). A series of factors participating in axial determination of the limb bud have been proposed, such as *Wnt7a* which is involved in D/V patterning, *Shh* which is specifying posterior identities, members of the *Fgf* family for distal outgrowth, *LMX1* for dorsalization and *En1* which is essential for limb ventralization (Dealy et al., 1996; Ohuchi et al., 1997). Another important group of genes are the *HOX* genes homolog to the *Drosophila HOM-C* (Krumlauf, 1994). Sections of embryos hybridized with *Irx3* suggest its possible involvement during establishment or maintenance of the D/V and P/D axes.

The initial *Irx1* expression in the limb bud from E10.5 onwards was limited to the region from which the AER arises, while later *Irx1* expression was located in the digits (not shown). The AER is involved in the separation of the digits (Williams et al., 1989). Experiments removing the AER led to truncated digits. Thus, *Irx1* may contribute to the process of digit formation.

3.5. Irx genes exhibit expression in concordance with Mash1 in the CNS and elsewhere

In *Drosophila* it has been found that the *Iro* genes positively control some of the *A/S-C* genes (Gómez-Skarmeta and Modolell, 1996).

Mash1 represents the only mammalian homolog of the *AS-C* genes with transcriptional activity during embryonic nervous system development. In analogy to the functional cascade in the fly, *Mash1* could be a potential target gene of mammalian *Irx* genes. *Mash1* is expressed in proliferating precursors in CNS and autonomic NS during prenatal mouse development (Guillemot and Joyner, 1993; Lo et al., 1994). At E9.5 the distribution of *Irx1*, *-2* and *-3* transcripts completely match the *Mash1* expression within the CNS in the mesencephalic roof, hindbrain and spinal cord. One day later, the *Irx* genes and *Mash1* are coexpressed in the diencephalon, tegmentum and in certain sensory ganglia. In addition, *Mash1* expression can be correlated with *Irx* gene activity in the developing lung. The spatial expression of *Irx* genes, which at least partially overlaps with *Mash1* expression in the mouse embryo, suggests a possible conservation of the regulatory genetic interaction from fly to mouse.

In particular, *Mash1* starts to be expressed at E9.5, and thus differs from the onset of *Irx* expression (Guillemot and Joyner, 1993). As a possible downstream target, also the mouse homolog to *Xash3* would be an interesting candidate for a role in neuronal induction (Zimmerman et al., 1993).

Further upstream regulatory genes for the *Drosophila Iro-C* locus have been reported (Gómez-Skarmeta and Modolell, 1996). Thus, a zinc-finger domain containing gene, *cubitus interuptus (ci)*, functioning as a segment polarity gene in *Drosophila* may regulate together with *dpp* the activity of the *Iro-C* genes. Homologs have been identified in *C. elegans (tral)*, mouse *(Gli1-3)* and human (Vortkamp et al., 1991; Schimmang et al., 1992; Hui et al., 1994).

Interestingly, our mouse *Irx* expression data reveal several parallels to the expression of putative upstream genes, the members of the *Gli*-family. The initial expression of the *Gli* genes is detected during gastrulation in the overlapping ectoderm and mesoderm and later with distinct patterns in the developing neural tube similar to the *Irx* expression. Moreover, the *Gli* genes show also a D/V patterning in the developing neural tube like the *Irx* genes. A naturally occurring *Gli3* mutation, the mouse extra-toes mutant, shows neural tube closure defects and skeletal malformations (Hui et al., 1994). Mutations in the human *Gli3* gene lead

to the developmental disorder GCPC (Greig-Cephalo-Polysyndactylie-syndrome) which has similar limb and craniofacial malformations (Vortkamp et al., 1991).

In conclusion, the sequence similarity of mouse *Irx* genes combined with their pattern of expression during development suggests both a structural and a functional correlation with *Drosophila Iroquois* genes. This notion is further supported by the similarity between the expression patterns of *Irx* genes and those of the putative mammalian homologs in the *Drosophila* signaling cascade.

4. Experimental procedures

4.1. cDNA analysis

A homeobox derived 700-bp probe from the *Drosophila ara* gene was used to screen a mouse E8.5 C57BL murine λgtlO poly (T)-primed cDNA library (kindly provided by Dr. Brigid Hogan) according to (Oliver et al., 1995). A total of 10^6 plaques were screened and 13 independent phages were isolated. Sequence analysis revealed that the 13 cDNA fragments contained three diverged murine *Iroquois* related genes.

Four cDNA clones represented the same homeobox comprising a region of ~1.7 kb. It was named *I*roquois-homeobo*x*-3 (Irx3). To expand the *Irx3* cDNA fragment a further 5′, an E14.5 randomly primed cDNA library (kindly provided by Dr. R. Wehr) was screened at high stringency using a 5′-probe excluding homeobox sequences. One clone extended the previously isolated cDNA around 700 bp in the 5′ direction. The *Irx3* cDNA has a total length of ~2.4 kb including an open reading frame encoding a 507 amino acid protein. The sequence directly upstream of the proposed initiation methionine agreed in all six bases with the 'Kozak consensus sequence' (Kozak, 1987).

Another set of four cDNA clones contained fragments of the *Irx1* gene and spanned a length of ~1.5 kb. The remaining three cDNAs belonged to the *Irx2* gene comprising in total ~2.2 kb. The translation start points of *Irx1* and *Irx2* have not yet been cloned.

4.2. Northern blot analysis

RNAs were extracted from E10.5–E17.5 NMRI embryos using the lithium chloride-urea method described by (Auffray and Rougeon, 1980). PolyA^+ RNA was isolated from total RNA using columns containing Poly(U) sepharose4B (Pharmacia). PolyA^+ RNA (3 μg) was separated in a 1.2% agarose-formaldehyde gel and transferred to a nylon membrane (Qiagen). Hybridizations with the *Irx1, -2* and *-3* specific probes were performed overnight at 42°C in 50% formamide, 1M sodium chloride, 1% SDS and 100 μg/ml salmon sperm DNA. Blots were sequentially washed in 2× SSC, 0.5% SDS (two times 30 min at 65°C) and in 0.1× SSC, 0.5%SDS (once for 30 min at 65°C).

4.3. In situ hybridization

The cloning of the murine *Irx* members from a E8.5 cDNA library implies expression during early stages of embryonic development. Whole mount in situ hybridizations (Wilkinson and Nieto, 1993) using in vitro probes deriving from regions outside of the conserved *Irx* homeobox were performed on mouse embryos from E6.5–E10.5. For each gene we used at least two different probes between 0.5–1.0 kb, and the detected patterns were identical. Sense RNA probes were used as negative controls in all experiments. Structures in the developing nervous system were named according to the atlas of (Alvarez-Bolado and Swanson, 1996).

Acknowledgements

We are especially grateful to Kamal Chowdhury for advice on various experimental procedures; Anastasia Stoykova, Barbara Meyer, Lydia Lemaire, Kenneth Ewan and Eva Bober for stimulating discussions on the manuscript. We wish to thank also Ralf Altschäffel for excellent photographic work and ClausPeter Adam for the illustration in Fig. 8. This work was supported by grants from the Deutsche Forschungsgemeinschaft (SFB No. 271) and from DGICYT to J. Modolell, by Fundacion Ramon Areces, by the Leibnitz program and in part by the European Union.

References

Allende, M.L., Weinberg, E.S., 1994. The expression pattern of two zebrafish achaete-scute homolog (ash) genes is altered in the embryonic brain of the cyclops mutant. Dev. Biol. 166, 509–530.

Alvarez-Bolado, G., Swanson, L.W., 1996. Developmental Brain Maps: Structure of the Emryonic Rat Brain. Elsevier, Amsterdam.

Auffray, C., Rougeon, F., 1980. Purification of mouse immunoglobulin heavy-chain messenger RNAs from total myeloma tumor RNA. Eur. J. Biochem. 107, 303–314.

Bellefroid et al., 1997. EMBO J., in press.

Campuzano, S., Modolell, J., 1992. Patterning of the Drosophila nervous system: the achaete-scute gene complex. Trends Genet. 8, 202–208.

Chitnis, A., Kintner, C., 1996. Sensitivity of proneural genes to lateral inhibition affects the pattern of primary neurons in Xenopus embryos. Development 122, 2295–2301.

Dealy, C.N., Clarke, K., Scranton, V., 1996. Ability of FGFs to promote the outgrowth and proliferation of limb mesoderm is dependent on IGF-I activity. Dev. Dyn. 206, 463–469.

Fekete, D.M., 1996. Cell fate specification in the inner ear. Curr. Opin. Neurobiol. 6, 533–541.

Ferreiro, B., Kintner, C., Zimmerman, K., Anderson, D., Harris, W.A., 1994. XASH genes promote neurogenesis in Xenopus embryos. Development 120, 3649–3655.

Ghysen, A., Dambly-Chaudiere, C., Jan, L.Y., Jan, Y.N., 1993. Cell interactions and gene interactions in peripheral neurogenesis. Genes Dev. 7, 723–733.

Goddard, J.M., Rossel, M., Manley, N.R., Capecchi, M.R., 1996. Mice with targeted disruption of Hoxb-1 fail to form the motor nucleus of the VIIth nerve. Development 122, 3217–3228.

Gomez-Skarmeta, J.L., Modolell, J., 1996. araucan and caupolican provide a link between compartment subdivisions and patterning of sensory organs and veins in the Drosophila wing. Genes Dev. 10, 2935–2945.
Gómez-Skarmeta et al., 1997. EMBO J., in press.
Guillemot, F., 1995. Analysis of the role of basic-helix-loop-helix transcription factors in the development of neural lineages in the mouse. Biol. Cell 84, 3–6.
Guillemot, F., Joyner, A.L., 1993. Dynamic expression of the murine Achaete-Scute homologue Mash-1 in the developing nervous system. Mech. Dev. 42, 171–185.
Hadrys et al., 1997. Development 125, in press.
Hui, C.C., Slusarski, D., Platt, K.A., Holmgren, R., Joyner, A.L., 1994. Expression of three mouse homologs of the Drosophila segment polarity gene cubitus interruptus, Gli, Gli-2, and Gli-3, in ectoderm- and mesoderm-derived tissues suggests multiple roles during postimplantation development. Dev. Biol. 162, 402–413.
Jan, Y.N., Jan, L.Y., 1994. Neuronal cell fate specification in Drosophila. Curr. Opin. Neurobiol. 4, 8–13.
Joyner, A.L., 1996. Engrailed, Wnt and Pax genes regulate midbrain-hindbrain development. Trends Genet. 12, 15–20.
Kageyama, R., Sasai, Y., Akazawa, C., Ishibashi, M., Takebayashi, K., Shimizu, C., Tomita, K., Nakanishi, S., 1995. Regulation of mammalian neural development by helix-loop-helix transcription factors. Crit. Rev. Neurobiol. 9, 177–188.
Keynes, R., Krumlauf, R., 1994. Hox genes and regionalization of the nervous system. Annu. Rev. Neurosci. 17, 109–132.
Kozak, M., 1987. An analysis of 5'-noncoding sequences from 699 vertebrate messenger RNAs. Nucleic Acids Res. 15, 8125–8148.
Krumlauf, R., 1994. Hox genes in vertebrate development. Cell 78, 191–201.
Lee, J.E., 1997. NeuroD and neurogenesis. Dev. Neurosci. 19, 27–32.
Leyns, L., Gómez-Skarmeta, J.L., Dambly-Chaudiere, C., 1996. iroquois: a prepattern gene that controls the formation of bristles on the thorax of Drosophila. Mech. Dev. 59, 63–72.
Lo, L., Guillemot, F., Joyner, A.L., Anderson, D.J., 1994. MASH-1: a marker and a mutation for mammalian neural crest development. Perspect. Dev. Neurobiol. 2, 191–201.
Lumsden, A., Krumlauf, R., 1996. Patterning the vertebrate neuraxis. Science 274, 1109–1115.
Mansour, S.L., Thomas, K.R., Capecchi, M.R., 1988. Disruption of the protooncogene int-2 in mouse embryo-derived stem cells: a general strategy for targeting mutations to non-selectable genes. Nature 336, 348–352.
Mansouri, A., Hallonet, M., Gruss, P., 1996. Pax genes and their roles in cell differentiation and development. Curr. Opin. Cell Biol. 8, 851–857.
McGinnis, W., Krumlauf, R., 1992. Homeobox genes and axial patterning. Cell 68, 283–302.
McNeill, H., Yang, C.H., Brodsky, M., Ungos, J., Simon, M.A., 1997. mirror encodes a novel PBX-class homeoprotein that functions in the definition of the dorsal-ventral border in the Drosophila eye. Genes Dev. 11, 1073–1082.
Moscoso del Prado, J., Garcia-Bellido, A., 1984. Genetic regulation of the Acheate-scute complex of Drosophila melanogaster. Roux's Arch. Dev. Biol. 193, 242–245.
Muskavitch, M.A., 1994. Delta-notch signaling and Drosophila cell fate choice. Dev. Biol. 166, 415–430.
Noden, D.M., Van de Water, T.R., 1992. Genetic analyses of mammalian ear development. Trends Neurosci. 15, 235–237.
Ohuchi, H., Shibusawa, M., Nakagawa, T., Ohata, T., Yoshioka, H., Hirai, Y., Nohno, T., Noji, S., Kondo, N., 1997. A chick wingless mutation causes abnormality in maintenance of Fgf8 expression in the wing apical ridge, resulting in loss of the dorsoventral boundary. Mech. Dev. 62, 3–13.
Oliver, G., Wehr, R., Jenkins, N.A., Copeland, N.G., Cheyette, B.N., Hartenstein, V., Zipursky, S.L., Gruss, P., 1995. Homeobox genes and connective tissue patterning. Development 121, 693–705.
Parks, A.L., Huppert, S.S., Muskavitch, M.A., 1997. The dynamics of neurogenic signalling underlying bristle development in Drosophila melanogaster. Mech. Dev. 63, 61–74.
Rivolta, M.N., 1997. Transcription factors in the ear: molecular switches for development and differentiation. Audiol. Neuro-Otol. 2, 36–49.
Rowitch, D.H., McMahon, A.P., 1995. Pax-2 expression in the murine neural plate precedes and encompasses the expression domains of Wnt-1 and En-1. Mech. Dev. 52, 3–8.
Ruben, R.J., Rapin, I., 1980. Plasticity of the developing auditory system. Ann. Otol. Rhinol. Laryngol. 89, 303–311.
Ruben, R.J., Van De Water, T.R., Rubel, E., 1986. The Biology of Change in Otolaryngology. Elsevier, Clearwater Beach, FL.
Schimmang, T., Lemaistre, M., Vortkamp, A., Ruther, U., 1992. Expression of the zinc finger gene Gli3 is affected in the morphogenetic mouse mutant extratoes (Xt). Development 116, 799–804.
Sommer, L., Shah, N., Rao, M., Anderson, D.J., 1995. The cellular function of MASH1 in autonomic neurogenesis. Neuron 15, 1245–1258.
Swanson, G.J., Howard, M., Lewis, J., 1990. Epithelial autonomy in the development of the inner ear of a bird embryo. Dev. Biol. 137, 243–257.
Tanabe, Y., Jessell, T.M., 1996. Diversity and pattern in the developing spinal cord. Science 274, 1115–1123.
Torres, M., Gomez-Pardo, E., Gruss, P., 1996. Pax2 contributes to inner ear patterning and optic nerve trajectory. Development 122, 3381–3391.
Treisman, J., Gonczy, P., Vashishtha, M., Harris, E., Desplan, C., 1989. A single amino acid can determine the DNA binding specificity of homeodomain proteins. Cell 59, 553–562.
Vervoort, M., Dambly-Chaudiere, C., Ghysen, A., 1997. Cell fate determination in Drosophila. Curr. Opin. Neurobiol. 7, 21–28.
Vortkamp, A., Gessler, M., Grzeschik, K.H., 1991. GLI3 zinc-fingel gene interrupted by translocations in Greig syndrome families. Nature 352, 539–540.
Wilkinson, D.G., Bhatt, S., McMahon, A.P., 1989. Expression pattern of the FGF-related proto-oncogene int-2 suggests multiple roles in fetal development. Development 105, 131–136.
Wilkinson, D.G., Nieto, M.A., 1993. Detection of messenger RNA by in situ hybridization to tissue sections and whole mounts. Methods Enzymol. 225, 361–373.
Wilkinson, D.G., Peters, G., Dickson, C., McMahon, A.P., 1988. Expression of the FGF-related proto-oncogene int-2 during gastrulation and neurulation in the mouse. EMBO J. 7, 691–695.
Williams, P.L., Warwick, R., Dyson, M., Bannister, L.H., 1989. Gray's Anatomy. Churchill Livingstone.
Zimmerman, K., Shih, J., Bars, J., Collazo, A., Anderson, D.J., 1993. XASH-3, a novel Xenopus achaete-scute homolog, provides an early marker of planar neural induction and position along the mediolateral axis of the neuraj plate. Development 119, 221–232.